7-1-2009

A High-Resolution Record of Atmospheric Dust Composition and Variability Since Ad 1650 from a Mount Everest Ice Core

S. Kaspari

Paul Andrew Mayewski
University of Maine - Main, paul.mayewski@maine.edu

M. Handley

Shichang Kang

S. Hou

See next page for additional authors

A High-Resolution Record of Atmospheric Dust Composition and Variability since A.D. 1650 from a Mount Everest Ice Core

S. KASPARI,*,+ P. A. MAYEWSKI,*,# M. HANDLEY,* S. KANG,#,@ S. HOU,# S. SNEED,* K. MAASCH,* AND D. QIN#

* *Climate Change Institute, and Department of Earth Sciences, University of Maine, Orono, Maine*
+ *Paul Scherrer Institute, Villigen, Switzerland*
# *State Key Laboratory of Cryospheric Science, Chinese Academy of Sciences, Lanzhou, China*
@ *Institute of Tibetan Plateau Research, Chinese Academy of Sciences, Beijing, China*

(Manuscript received 7 March 2008, in final form 21 January 2009)

ABSTRACT

A Mount Everest ice core analyzed at high resolution for major and trace elements (Sr, Cs, Ba, La, Ce, Pr, Nd, Sm, Eu, Tb, Dy, Ho, Er, Tm, Yb, Lu, Bi, U, Tl, Al, S, Ca, Ti, V, Cr, Mn, Fe, Co) and spanning the period A.D. 1650–2002 is used to investigate the sources of and variations in atmospheric dust through time. The chemical composition of dust varies seasonally, and peak dust concentrations occur during the winter–spring months. Significant correlations between the Everest dust record and dust observations at stations suggest that the Everest record is representative of regional variations in atmospheric dust loading. Back-trajectory analysis in addition to a significant correlation of Everest dust concentrations and the Total Ozone Mapping Spectrometer (TOMS) aerosol index indicates that the dominant winter sources of dust are the Arabian Peninsula, Thar Desert, and northern Sahara. Factors that contribute to dust generation at the surface include soil moisture and temperature, and the long-range transport of dust aerosols appears to be sensitive to the strength of 500-mb zonal winds. There are periods of high dust concentration throughout the 350-yr Mount Everest dust record; however, there is an increase in these periods since the early 1800s. The record was examined for recent increases in dust emissions associated with anthropogenic activities, but no recent dust variations can be conclusively attributed to anthropogenic inputs of dust.

1. Introduction

Assessing the dust loading of the atmosphere is important because dust aerosols can affect climate, global biogeochemical cycles, the hydrologic cycle, and human health. Dust aerosols impact the climate system by altering the earth's radiative balance (Solomon et al. 2007). The presence of mineral dust scatters and partly absorbs incoming solar radiation, absorbs and reemits outgoing longwave radiation, and can thus affect surface temperatures (Miller and Tegen 1998). Estimating the dust radiative impact is complex because the dust burden pattern is spatially and temporally variable: dust sources and sinks are not uniformly distributed, and the lifetime of mineral aerosols is less than a few weeks (Duce 1995). Dust also plays a large role in global biogeochemical cycles, as wind-transported dust is a major source of iron and other limiting nutrients that control ocean productivity (Jickells et al. 2005). Additionally, atmospheric dust can also affect cloud properties and precipitation patterns (Rosenfeld et al. 2001), and small dust particles are harmful to human respiratory health (Griffin and Kellogg 2004).

The largest and most persistent sources of dust are from desert regions in the Northern Hemisphere, including North Africa, the Arabian Peninsula, central Asia, and China (Prospero et al. 2002). The dust loading of the atmosphere is known to be temporally variable. In addition, the frequency and intensity of dust events may increase because of human activities including agriculture, overgrazing, deforestation, unpaved roads, construction, and military activities in desert regions (Tegen et al. 2004; Mahowald et al. 2004). Records of past dust variability from these arid regions are essential to put these potential changes into context and to assess the

Corresponding author address: Susan Kaspari, Paul Scherrer Institut, Labor für Radio- und Umweltchemie, CH-5232 Villigen PSI, Switzerland.
E-mail: susan.kaspari@psi.ch

DOI: 10.1175/2009JCLI2518.1

impact of dust aerosols on the climate system, biogeochemical and hydrological cycles, and human health.

Some of the earliest written records of dust storm activity are recorded in ancient Chinese literature, and historical records have been used to reconstruct dust storm frequency since A.D. 300 (Goudie and Middleton 1992; Zhang 1985). These historical records demonstrate the occurrence of Asian dust storms through time but do not provide a continuous record. Detailed meteorological records of dust storm activity in China and the surrounding regions are available since the 1950s (National Climate Center, China Meteorological Administration), and satellite observations provide a record of aerosol optical depth since the late 1970s (Torres et al. 1998, 2002). The station and satellite data have greatly improved our understanding about recent dust storm activity, including their timing, transport, and composition. However, the limited temporal coverage of these measurements is insufficient to understand changes in dust storm activity prior to the 1950s and does not allow for modern dust events to be put into a longer historical context.

Ice cores recovered from appropriately chosen sites are an ideal archive for reconstructing past atmospheric dust aerosol loading, transport, and chemical composition prior to the instrumental record. Ice cores provide high-resolution, well-preserved, multiparameter archives of the atmospheric signature from remote regions, including information about past temperature, precipitation, atmospheric circulation, and atmospheric chemistry. The glaciated, high-elevation mountain regions in Asia are located downwind or in the vicinity of the largest dust sources on earth. Thus, ice cores from these regions provide invaluable natural archives of past dust variability and composition. Himalayan glaciers have previously been identified as among the best locations for retrieving ice cores that provide detailed records of the long-range transport of Asian dust (Wake et al. 1993, 1994). Asian ice cores to date have predominantly been analyzed for major ions and stable isotopes (Kang et al. 2002; Thompson et al. 2000). However, by analyzing these ice cores for more chemical variables, the chemical signature can be better defined. Kreutz and Sholkovitz (2000) analyzed an ice core from the Tian Shan for major (Al, Fe, Ca, and S) and rare earth elements and demonstrated that, by including additional dust-related elements, it is possible to discern distinct mineral deposits (loess, calcium carbonate, and gypsum) associated with changes in atmospheric circulation and dust transport from multiple sources. However, thus far the geographic source regions of the dust deposited in ice cores has not been definitively identified. Additional research is needed to identify the sources of dust, the processes that control dust generation in these dust regions, and the meteorological conditions that enable the long-range transport of dust (Prospero et al. 2002).

Here a glaciochemical record from a Mount Everest ice core record analyzed for more chemical parameters than any other Asian ice core, including trace and major elements (Sr, Cs, Ba, La, Ce, Pr, Nd, Sm, Eu, Tb, Dy, Ho, Er, Tm, Yb, Lu, Bi, U, Tl, Al, S, Ca, Ti, V, Cr, Mn, Fe, Co), major ions (Na^+, K^+, Mg^{2+}, Ca^{2+}, Cl^-, NO_3^-, SO_4^{2-}), and stable isotopes (δD) is presented. The trace element record is used to examine variations in the composition and concentration of atmospheric dust through time, the dominant dust source regions and atmospheric transport pathways, the environmental controls on dust generation, and if recent human activities have increased the dust burden of the mid–upper troposphere over the Himalayas.

2. Site description and methods

In 2002 a joint Chinese Academy of Sciences and University of Maine Climate Change Institute team recovered a 108-m ice core drilled to bedrock from the col of the East Rongbuk glacier located on the northeast ridge of Mount Everest (28.03°N, 86.96°E, 6518 m ASL) (Fig. 1). Climatically, Mount Everest lies at the boundary of continental air masses associated with the westerlies and marine air masses associated with the summer South Asian monsoon (Kaspari et al. 2007). The mean accumulation rate at the site as calculated from density profiles and annual layer thicknesses is ~50 cm water equivalent yr^{-1} (Kaspari et al. 2007, 2008).

Standard clean procedures were used during retrieval of the ice core, and the ice core was shipped frozen to the University of Maine for processing and analyses. The ice was melted into discrete samples at 3–4-cm resolution using an aluminum melter head with the University of Maine's continuous melter system. The melter head splits the meltwater into two different channels: meltwater from the outer portion of the ice core is collected in an outer channel for isotope analyses, and meltwater from the innermost section of the ice core is collected in an inner channel for major ion and trace element analyses. Osterberg et al. (2006) provide detailed information on the melter system and analyses. The ice core was analyzed at the University of Maine for major ions (Na^+, K^+, Mg^{2+}, Ca^{2+}, Cl^-, NO_3^-, SO_4^{2-}) via ion chromatography, stable isotopes (δD) via mass spectrometry, and trace elements (Na, Mg, Al, S, Ca, Ti, V, Cr, Mn, Fe, Co, Sr, Cs, Ba, La, Ce, Pr, Nd, Sm, Eu, Tb, Dy, Ho, Er, Tm, Yb, Lu, Tl, Bi, U) via inductively coupled plasma sector field mass spectrometry (ICP-SFMS). The ICP-

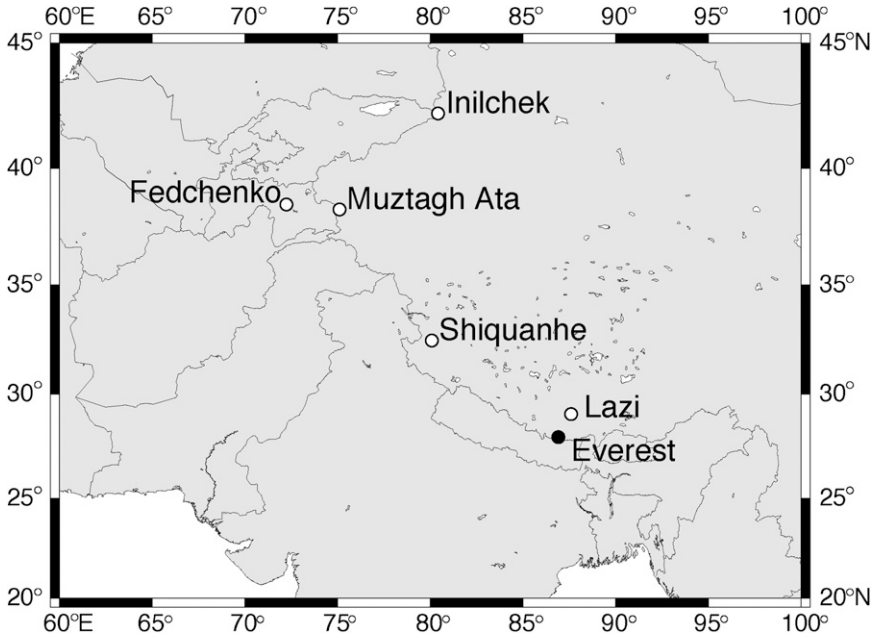

FIG. 1. Location map of the Mount Everest (black dot), Muztagh Ata, and Inilchek ice core drill sites, and the Shiquanhe and Lazi dust stations.

SFMS samples were acidified to 1% HNO_3, allowed to react with the acid for seven days, and then frozen until analyzed. Just prior to analysis the samples were spiked to contain 1 ppb indium as an internal standard.

The ice core was annually dated using seasonal variations of major ions, trace elements, and δD (Fig. 2), and the time scale was verified using volcanic horizons, including Mount Pinatubo (1991), Agung (1963), and Tambora (1815). Kaspari et al. (2007, 2008) provide detailed information on the depth–age scale. Herein the record is focused on the time period since A.D. 1650.

3. Results and discussion

a. Intersite comparison of element concentrations

A comparison of the median concentrations in the Mount Everest ice core with trace element records from other Asian ice cores [Inilchek, Tian Shan (Kreutz and Sholkovitz 2000); Muztagh Ata (Li et al. 2006)] suggests that concentrations of most elements are lower at Mount Everest (Table 1). Soluble major ion concentrations at Inilchek and Everest were analyzed via the same methods; however, there are differences between sites in trace element sample preparation and analytical methods. Trace element samples were completely digested at Inilchek (Kreutz and Sholkovitz 2000), whereas the Muztagh Ata samples were acidified with HNO_3 for 3–5 h prior to analysis (Li et al. 2006), and the Everest samples were acidified to 1% HNO_3 for seven days prior to analysis. Thus, the trace element concentrations reported at Inilchek are representative of total (soluble and insoluble) sample concentrations, while concentrations reported for Muztagh Ata and Everest are representative of the soluble plus a portion of the insoluble element concentrations. A comparison of soluble major ion concentrations at Everest and Inilchek indicates that ion concentrations are considerably higher at Inilchek. Concentrations of most trace elements at Inilchek are more than a magnitude higher than concentrations at Everest. This difference is larger than expected solely because of differences in analytical methods (e.g., total Ca concentrations at Inilchek are only twice as high as soluble Ca^{2+}). Thus, trace element concentrations are likely considerably lower at Mount Everest. This is consistent with previous work that demonstrated that concentrations of major ions in snow and ice are highest in northern and western regions of the Tibetan Plateau, which are surrounded by large desert basins that are a large source of dust aerosols. In contrast, major ion concentrations in the Himalayas are considerably lower (Wake et al. 1993).

b. Seasonal timing of dust deposition

There are large seasonal variations in the trace element concentrations at Everest, characterized by a distinct peak in dust elements (e.g., Al, Ti, Fe, Yb) once a year coincident with increased atmospheric dust concentrations (Fig. 2). This is consistent with previous

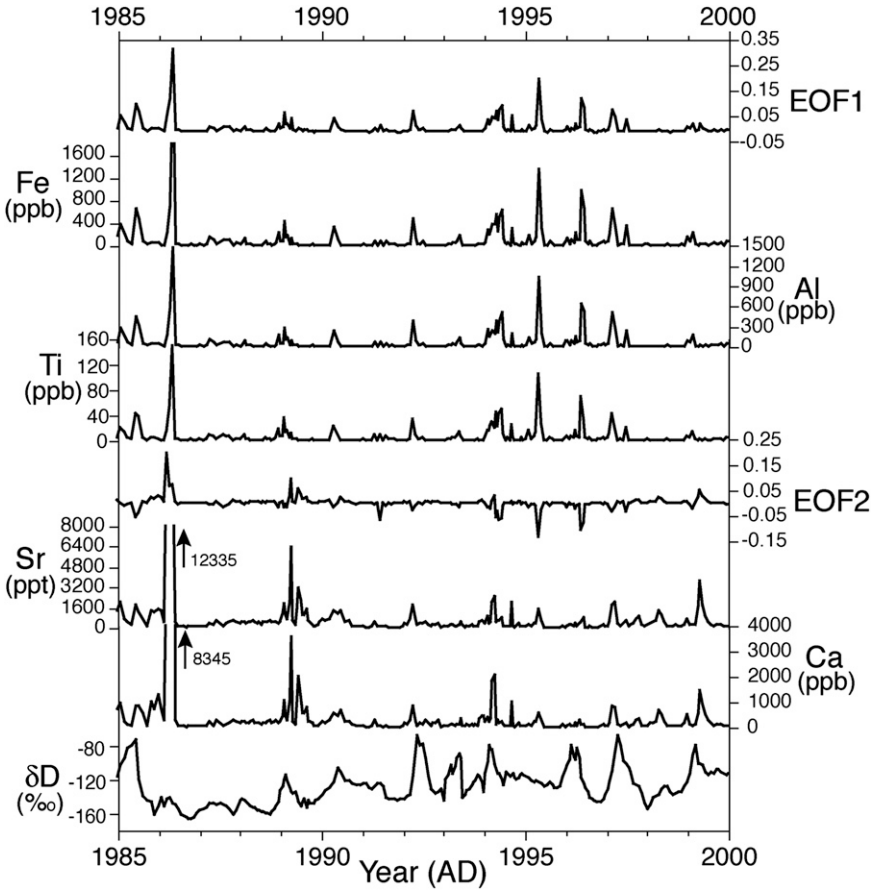

FIG. 2. High-resolution Mount Everest ice core data showing seasonal variations in EOF1, Fe, Al, Ti, EOF2, Sr, Ca, and δD.

major ion research at Mount Everest (Kang et al. 2004, 2002; Kaspari et al. 2007). Dust storm activity peaks during winter–spring because of unstable atmospheric conditions and strong winds. These atmospheric conditions enable dust aerosols to ascend rapidly to high altitudes after which they can be transported long distances (Prospero et al. 1989). Dust station data from Lazi (National Climate Center, China Meteorological Administration) near Mount Everest verifies this strong seasonal cycle, with peak dust activity occurring during December–March and minimal dust activity from June to September during the summer monsoon season (Fig. 3).

Ca and Sr generally peak at the same time as Al, Ti, and Fe; however, at times (e.g., during the late 1990s) there are peaks in Ca and Sr when Al, Ti, and Fe concentrations are low (Fig. 2). This suggests that there are sources of Ca and Sr unique to the dominant source of Al, Ti, and Fe. Empirical orthogonal function (EOF) analysis conducted on the high-resolution Everest trace element time series covering the period 1650–2002 confirms that there are two disparate sources of Ca and Sr (Table 2). EOF1 is loaded predominantly with those elements that peak during the winter–spring dust season (Al, Ti, Fe, V, Mn, Tl, Ba, Cs, Co, Yb, U, and Cr, and to a lesser degree with Ca, Sr, and Bi). Thus, EOF1 is representative of the winter–spring dust input. EOF2 is loaded with Ca and Sr and is representative of dust inputs that are unique to the EOF1 dust signal but still peak in winter–spring. EOF3 is loaded with Bi related to volcanic inputs and is discussed in greater detail by Kaspari et al. (2007).

Previous research on atmospheric aerosols in the vicinity of Mount Everest at Gongga (29.48°N, 91.57°E) and Lhasa (29.70°N, 91.15°E) found that the mass-particle size distributions of Ca, K, and Si are larger than Al, Fe, and Ti. This suggests that particles enriched in Ca, K, and Si are more strongly affected by local sources, whereas particles enriched in Al, Fe, and Ti are from more distal sources (Zhang et al. 2001). Similarly, an aerosol study of particle size fractions at the Pyramid Laboratory–Observatory in the Khumbu Valley south of Mount Everest found that particles enriched in Ca are of a

TABLE 1. Median element and major ion concentrations from ice cores from Mount Everest (this work), Inilchek (Kreutz et al. 2000), and Muztagh Ata (Li et al. 2006). See text for details regarding analytical differences between sites. IC = ion chromatography.

Element	Units	Everest 1650–2002	Everest 1950–2002	Muztagh Ata 1950s–2000	Everest 1992–2002	Inilchek 1992–98
Sr	ppt	320.0	371.2	2600	192.8	
Cs	ppt	60.0	102.0	25	38.5	
Ba	ppt	306.8	343.8	1600	210.9	
La	ppt	13.9	15.9		6.54	245.3
Ce	ppt	31.0	34.1		15.04	650.2
Pr	ppt	3.8	4.4		1.80	62.9
Nd	ppt	15.7	17.4		7.31	208.1
Sm	ppq	3900	4600		2000	37 800
Eu	ppq	800	1000		500	9300
Gd	ppq	1800	3000		1300	32 900
Tb	ppq	600	700		300	4600
Dy	ppq	3400	4100		1900	28 800
Ho	ppq	600	800		300	4900
Er	ppq	1600	2200		900	13 000
Tm	ppq	200	300		100	
Yb	ppq	1300	1800		800	11 900
Lu	ppq	200	300		100	1800
Bi	ppt	2.6	5.4	6	2.2	
U	ppq	7400	19 000		13 300	
Tl	ppt	1.3	1.7		0.9	
Al	ppb	40.1	40.1	87.1	22.0	418.6
S	ppb	9.7	13.5		18.2	171.5
Ca	ppb	95.0	153.3		84.0	2073.9
Ti	ppt	3557.6	4624.4		1730.1	
V	ppt	80.6	97.1		48.8	801.0
Cr	ppt	85.2	95.4		56.1	958.4
Mn	ppt	1404.6	1744.9	6200	1246.2	6871.1
Fe	ppb	58.2	57.8		28.8	231.4
Co	ppt	28.8	35.9		25.1	2284.3
Na IC	ppb	8.6	8.2		7.0	98.5
K IC	ppb	5.0	6.2		4.9	23.4
Mg IC	ppb	5.6	5.2		2.7	38.3
Ca IC	ppb	106.6	122.1		67.1	899.4
Cl	ppb	12.6	13.3		11.1	151.6
NO3	ppb	89.5	99.1		76.2	258.8
SO4	ppb	42.2	45.1		37.5	417.0

larger size fraction than particles enriched in Fe (Giaveri et al. 2005).

The differences in particle size and input timing of Fe and Ca leads us to suggest that Fe (and similar elements strongly loaded on EOF1) are representative of distal dust sources that peak during winter–spring, whereas the EOF2 dust signal is representative of a more proximal, background dust signal. The most likely source for the EOF2 signal is regional Ca- and Sr-rich carbonates. For the following analyses Fe is used as a tracer for distal dust sources.

c. *Seasonal differences in the dust chemical composition*

Scatterplots and element ratios are used to further differentiate the sources of the elements and to investigate variations in the dust chemical composition with changing concentration. A scatterplot of Fe and Ti concentrations shows strong coherence ($R^2 = 0.96$), and the Ti/Fe ratio does not change with Fe concentration. This suggests that Fe and Ti have the same source (Fig. 4). Conducting the same analysis using Fe as the comparative element, similar results were found for the other elements heavily loaded (greater than 85% variance) on EOF1 (Table 2). Conversely, a scatterplot of Fe and Ca has a ''shotgun'' pattern, indicating multiple sources of one of these elements, namely, Ca. Furthermore, the Ca/Fe ratio is highest at low Fe concentrations. This is in agreement with our previous findings: at low Fe concentrations there are relatively greater Ca inputs from proximal dust sources, whereas at high Fe concentrations the Ca/Fe signal is dominated by distal dust sources. Similar results were found for Sr. A possible source for the Ca inputs when Fe concentrations are low (i.e.,

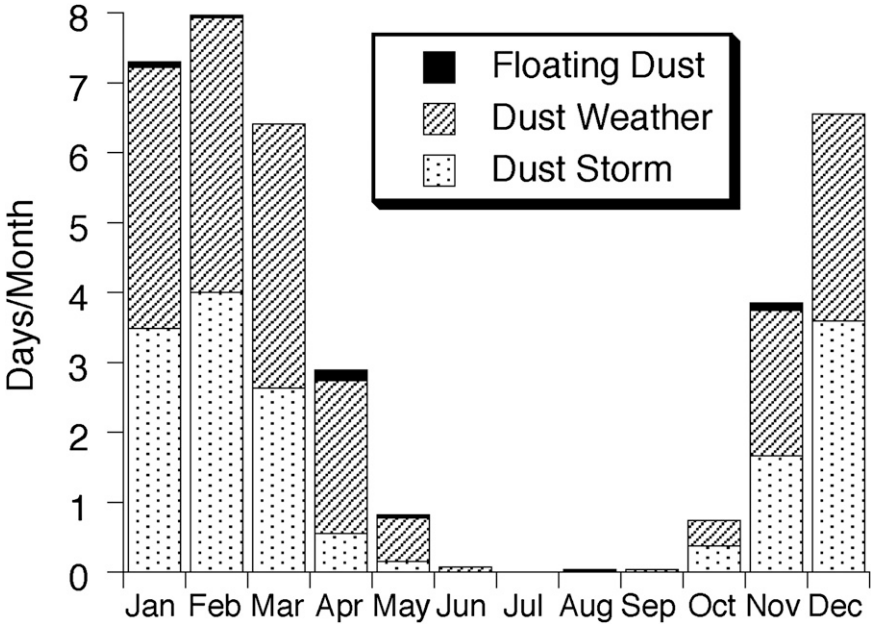

FIG. 3. Mean monthly dust observations from Lazi station.

during nonwinter months) are mesoscale valley winds that are strongest during summer (Song et al. 2007).

d. Geographic sources of dust

Periods of high Everest Fe and Ti concentrations are similar to periods of peak dust storm (strong and turbulent wind, horizontal visibility is <1 km) and dust weather (moderate wind, horizontal visibility is ~1–10 km) activity from the Shiquanhe and Lazi stations, most notably from 1979 to 1986 (Figs. 1, 6) (National Climate Center, Chinese Meteorological Administration). Shiquanhe station is selected because it has the longest continuous record of dust observations (1960–present) and is located upwind of Mount Everest, and Lazi station is chosen because of its close proximity to Mount Everest. There are notable differences in the dust observations from the Shiquanhe and Lazi stations (Fig. 5). Shiquanhe, located in an arid region of the western Tibetan Plateau, has more frequent occurrences of dust storms and dust weather year-round because of inputs from local dust sources. In contrast, dust inputs at Lazi peak during the winter and are low during the summer monsoon season, similar to the dust input timing at Mount Everest (Figs. 2, 3). There are differences between the station dust observations and Everest dust record because of differences in local dust sources, elevation, and atmospheric dust transport; however, the similarity in the ice core and station dust data, particularly in the early 1980s, suggests that the Mount Everest ice core record provides a proxy for regional dust loading. This is validated by significant correlations of the Mount Everest dust and the Lazi and Shiquanhe station dust data: the mean annual Mount Everest Fe record is significantly correlated with the annual station dust records (days of dust storms plus dust weather) at the Shiquanhe ($r = 0.36$, $n = 41$, $p < 0.05$) and Lazi stations ($r = 0.55$, $n = 25$, $p < 0.001$). That the Everest dust record is more strongly correlated with the Lazi station is not surprising, as Lazi is located closer to Everest than Shiquanhe. We would like to compare the

TABLE 2. EOF analysis on the high-resolution Mount Everest trace elements from the period 1650–2002.

	Dust	Background dust	Volcanic
	EOF1	EOF2	EOF3
	75.4	9.9	4.9
Sr	40.1	53.2	2.5
Cs	88.9	−0.2	−0.3
Ba	88.9	−0.3	0.1
Yb	79.4	7.4	0.0
Bi	28.2	−13.2	53.8
U	69.2	−0.2	0.2
Tl	93.6	−0.6	−1.7
Al	92.0	−2.3	−3.2
Ca	36.9	57.5	1.7
Ti	90.7	−1.9	−3.3
V	93.3	−1.4	−2.1
Cr	57.8	−3.8	4.1
Mn	88.2	1.1	0.0
Fe	90.0	−4.3	−0.1
Co	93.4	−1.7	−1.1

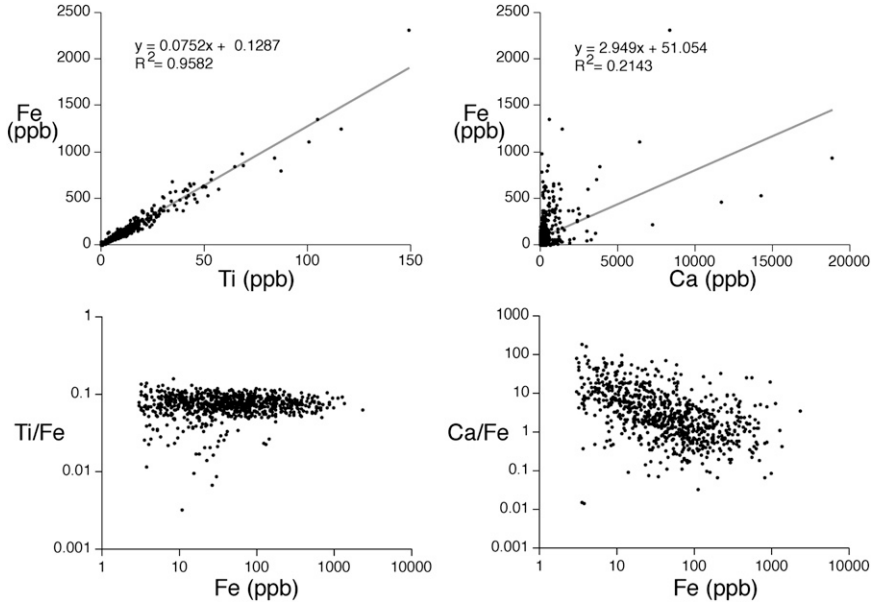

FIG. 4. Scatterplots and element ratios demonstrating that Fe and Ti have the same source, whereas relative contributions of Fe and Ca vary with concentration, suggesting different source inputs.

Everest dust records with dust observations from a similar elevation; however, no such record exists.

Satellite observations provide another method to investigate the dust loading of the atmosphere on much larger spatial scales and over seasonal to interannual time periods. The Total Ozone Mapping Spectrometer (TOMS) sensor on the *Nimbus-7* and *Earth Probe* satellites has been used to infer an absorbing aerosol index (AI) from measurements of UV radiances (Torres et al. 1998, 2002). The AI increases with both the amount of absorbing aerosol in the atmospheric column and the height of the aerosol layer and decreases from sulfate and other reflective aerosols in the column. Thus, spatial and temporal variations in the TOMS AI can result from changes in dust concentrations, the height of the dust layer, and/or the presence of other aerosols (Torres et al. 1998; Prospero et al. 2002; Mahowald and Dufresne 2004). Previous studies have used the TOMS data to map the global distribution of major atmospheric dust sources (Prospero et al. 2002; Washington et al. 2003). A comparison of Everest annual Fe to the TOMS AI (1978–93: ftp://jwocky.gsfc.nasa.gov/pub/nimbus7/data; 1996–2005: http://toms.gsfc.nasa.gov/eptoms/ep_v8.html) indicates that Fe is significantly correlated with the TOMS AI in January (1979–93, 1997–2001, $n = 20$, $r = 0.63$, $p > 0.005$) over the northern Arabian Peninsula and to a lesser degree the Thar Desert and the northern Sahara (Fig. 6a). There is a positive association between the annual Everest Fe and December and February TOMS AI in the same regions, but the correlation is strongest in January. The same analysis was done excluding the years 1983 and 1992–93 because the AI may not be representing variations in absorbing aerosols because of aerosol inputs from the El Chichón and Mount Pinatubo volcanic eruptions, respectively, and the 1996–2001 period because of potential differences between the *Nimbus-7* (1979–93) and *Earth Probe* (1997–2005) TOMS AI calibrations. In all cases Everest Fe is significantly correlated with the TOMS AI over the Arabian Peninsula and northern Sahara. This suggests that these are important sources of dust aerosols transported to Everest during winter–spring. The mean annual global distribution of the TOMS AI provides further support that the Arabian Peninsula, Thar Desert, and northern Sahara are important sources of aerosols (Prospero et al. 2002; Washington et al. 2003) (Fig. 6b). However, because the TOMS is a measure of the AI over the entire column, the AI may reflect dust being transported over a region rather than the ground source of the dust. Nevertheless, the location of peak surface observed dust storm frequencies in southwest Asia are consistent with the likely dust source regions identified above (Middleton 1986) (Fig. 6). The timing of the Everest Fe–TOMS AI correlation being strongest in winter is significant, as this is the period of peak dust activity in the Everest region (Fig. 3). Dust storm activity in the dust source regions tends to peak in the spring (Middleton 1986; TOMS AI). That peak dust

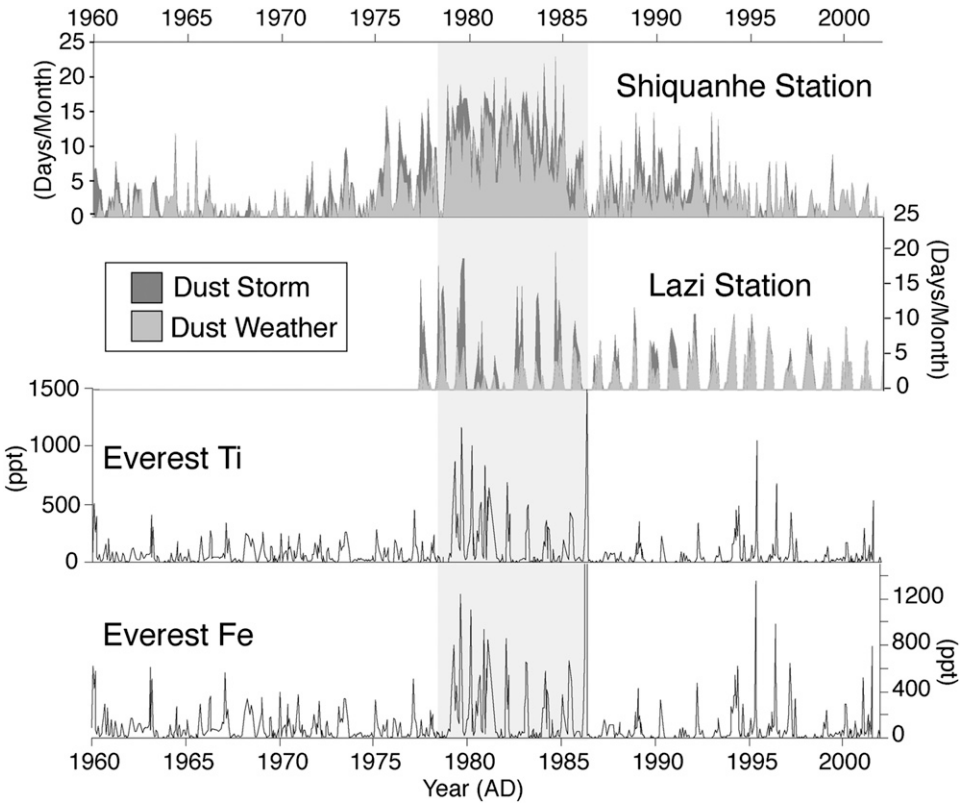

FIG. 5. Dust variability from station dust data (Chinese Meteorological Administration), and the Mount Everest ice core glaciochemical record. A dust storm day has strong and turbulent wind and horizontal visibility is <1 km, whereas a dust weather day has moderate winds and horizontal visibility is ~1–10 km.

deposition occurs during the winter months in the Everest region indicates that, in addition to dust emissions in source regions, the atmospheric transport of dust aerosols is an important control on the concentrations of dust deposited at Mount Everest. This is discussed further in the following section. Negative correlations in the tropical oceans are likely due to an increasing trend in the TOMS AI in these regions, concurrent with a decrease in Everest Fe. The TOMS AI in these oceans regions is very low (Fig. 6b), thus the inverse correlation is thought to be a statistical artifact.

Seven-day (the period typical of the residence time of dust particles in the atmosphere) back-trajectory analysis was conducted using the Hybrid Single-Particle Lagrangian Integrated Trajectory (HYSPLIT) model from the National Oceanic and Atmospheric Administration (NOAA). Back trajectories were run every 6 h for the 10 highest and 10 lowest dust years during January and February (total ~4700 trajectories). Back-trajectory frequency analysis, which creates a 1° gridded file representing the trajectory frequency at each grid point, demonstrates that the westerlies dominate atmospheric circulation in this region during the winter (Fig. 7). Additionally, the analysis shows the occurrence of trajectories over the high dust regions identified by the TOMS analysis (Fig. 6), demonstrating the presence of pathways by which dust aerosols from these regions can be transported to Mount Everest. The back-trajectory analysis is discussed in further detail below.

e. Controls on dust variability

Factors that can affect the dust loading of the atmosphere, and hence dust deposition at Mount Everest, include the aridity and wind conditions in the dust source regions that control dust generation and dust entrainment into the mid–upper troposphere and the strength and pathway of the westerlies that control long-range dust transport. Cropland and natural vegetation coverage can also act as a control on dust aerosol emissions but are not considered here because interannual variations in vegetation coverage are thought to not significantly impact dust emissions in the dust source regions under consideration (Engelstaedter et al. 2003; Tegen et al. 2004; Zender and Kwon 2005).

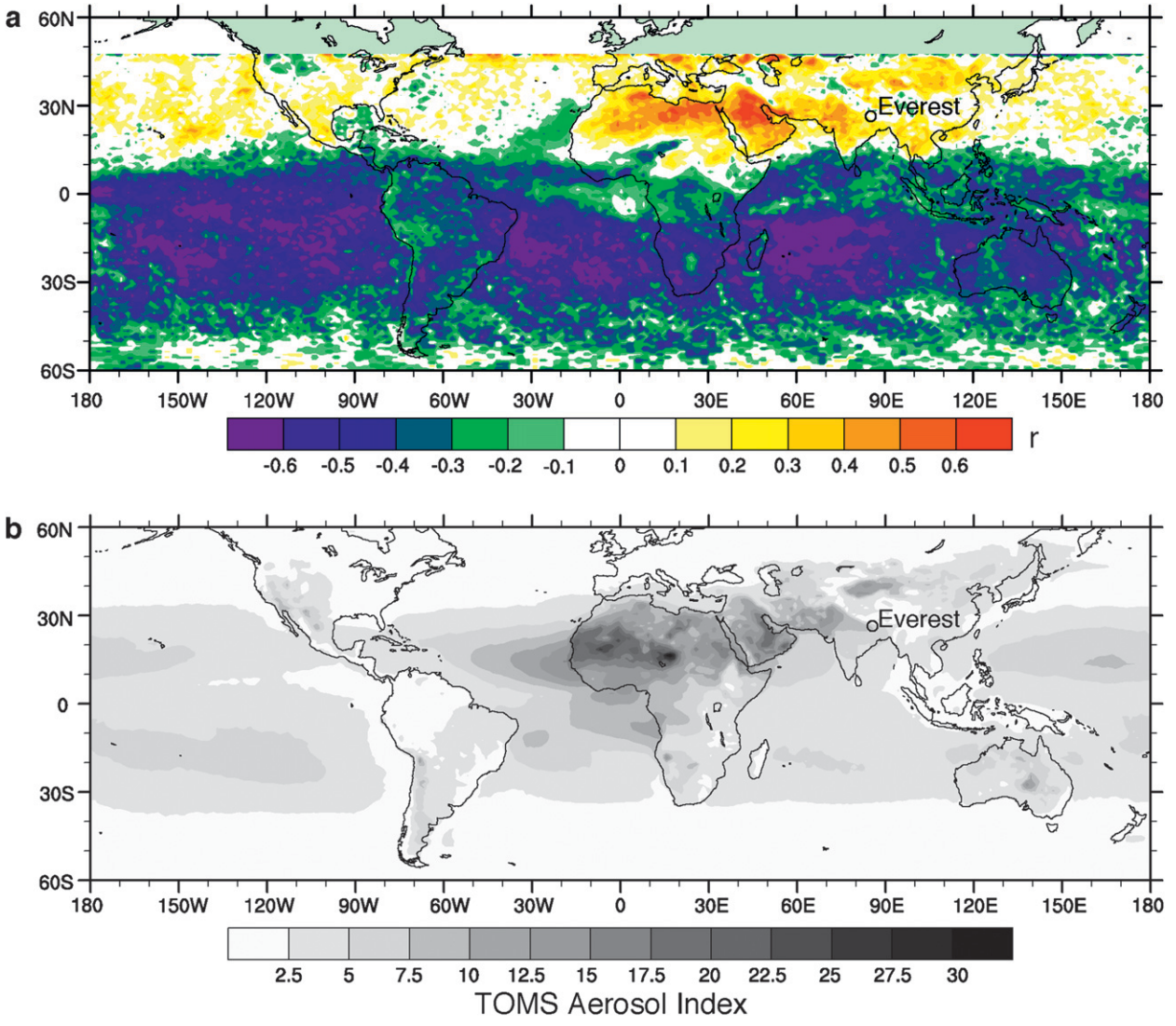

FIG. 6. (a) Correlation of January TOMS AI and mean annual Everest Fe from 1979 to 2001. (b) Mean annual TOMS AI (×10).

Aridity and wind conditions in the dust source regions as identified by the TOMS analysis are investigated (Fig. 6) with a focus on the winter months (January–February) because this is the peak period for dust deposition in the Everest region (Fig. 3). Figure 8a shows the National Centers for Environmental Prediction (NCEP) reanalysis mean precipitation rate, soil moisture, surface temperature, and surface wind speed during winter from 1948 to 2002 and the associated anomalies (relative to the 1968–96 NCEP climatology; Kalnay et al. 1996) during the 10 highest and lowest dust years (as defined by the mean annual Fe concentrations). The mean precipitation rate is extremely low in areas with a high TOMS AI (<0.5 mm day^{-1}) (Fig. 8a). The precipitation rate does not deviate substantially from the mean climatology during years of high or low dust concentration, with the exception of some regions of Iran where precipitation is anomalously low (high) during high (low) dust years. Equivalent results were found using data from the Global Precipitation Climatology Project (GPCP) during the period 1979–2001. NCEP soil moisture is anomalously high in years with low dust concentrations, which could lead to decreased dust aerosol production. However, it is important to note that the NCEP soil moisture is a model-derived value dependent upon the land surface model and model-generated precipitation as opposed to soil moisture observations, thus there is inherent uncertainty in these results. Temperature is anomalously high during high dust years, which could result in more arid conditions and increased dust emissions (Fig. 8a). Although not definitive, these results do suggest greater dust emissions during relatively warm and/or dry years.

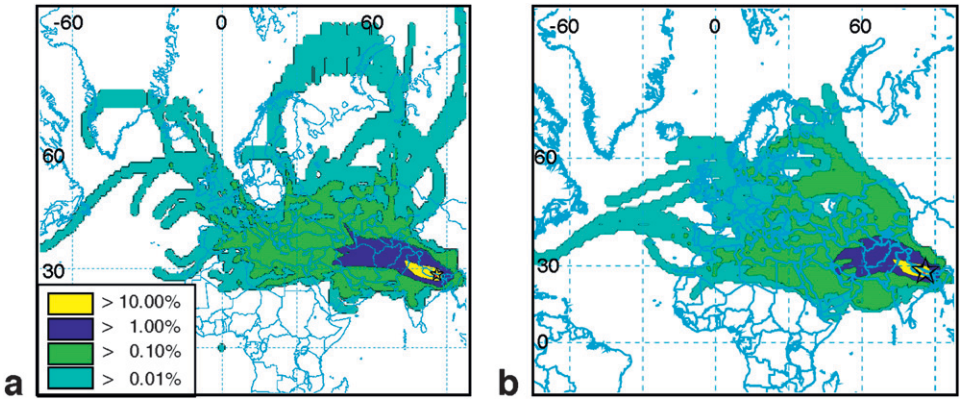

FIG. 7. Frequency plot of seven-day back trajectories for January and February for (a) the 10 highest and (b) the 10 lowest dust years between 1948 and 2002 using HYSPLIT and the NCEP reanalysis. Back trajectories were run every 6 h.

Surface scalar wind speed in the dust source regions may also be a potential indicator of surface turbulence that could entrain dust particles into the mid–upper troposphere. Surface wind speed anomalies in high dust years are spatially variable but do not deviate substantially from the 1968–96 climatology. Interestingly, surface wind speed anomalies are slightly higher than average in low dust years, contrary to what might be expected. Possible explanations for this include 1) factors such as precipitation, soil moisture, temperature, and vegetation are a larger control on atmospheric dust entrainment than wind speed, and/or 2) the conditions that are most likely to result in dust entrainment are episodic and usually occur over short time periods. These episodic events may not be captured by the monthly averaged wind speed and the relatively coarse time resolution of dust deposition as recorded in the ice core precludes identification of hourly to daily-scale events.

The influence of atmospheric circulation on the transport of dust aerosols to the Mount Everest core site is assessed by examining associations between pressure and zonal winds from the NCEP reanalysis and the Mount Everest mean annual Fe time series (representative of distal dust sources). Zonal winds are strongest during the winter months and track over the northern Sahara, Arabian Peninsula, and Thar Desert, enabling dust transport from these regions to Mount Everest (Fig. 8).

In years with high (low) Fe concentrations, surface pressure is anomalously high (low) in the region of the Icelandic low and, to a lesser extent, low (high) in the Atlantic subtropical high pressure center. This pressure pattern is equivalent to the North Atlantic Oscillation (NAO), with high (low) dust years occurring under the positive (negative) phase of the North Atlantic Oscillation. This suggests that dust transport to Mount Everest is teleconnected to North Atlantic conditions as expected because of the association of pressure in this region with the westerlies. Generally, a weaker Icelandic low (negative NAO) results in a more zonal atmospheric flow, while a deeper Icelandic low (positive NAO) results in more meridional flow (Hurrel et al. 2003). Indeed, 500-mb zonal wind anomalies during high (low) dust years indicate an intensification (weakening) of the westerlies focused at 30°N. This is consistent with the back-trajectory frequency plot for frequencies greater than 0.1% (Fig. 7). In high dust years, there is a slight increase in the frequency of trajectories in regions farther to the west of Everest relative to low dust years, suggesting intensified zonal winds during high dust years. However, an inherent uncertainty in the back-trajectory analysis is that it is not known during which times (i.e., which trajectories) dust is transported to Mount Everest. Thus, the back-trajectory analysis provides a cursory estimate of dust transport to Mount Everest.

Despite mean winter zonal winds being stronger hemispherically in high dust years, winds in the region from the northeast Sahara to Everest are actually slightly weaker in high dust years and stronger in low dust years (Fig. 8b). This provides additional support that episodic synoptic-scale conditions may be a larger control on dust entrainment and transport than mean conditions over monthly–seasonal time periods.

f. Dust variability since A.D. 1650

Periods of high dust concentrations occur throughout the 350-yr Mount Everest ice core record. However, there is an increase in periods with high Fe concentrations (and EOF1) since the early–mid-1800s (Fig. 9), suggesting an increase in atmospheric dust concentrations in the Everest and upwind regions since this time.

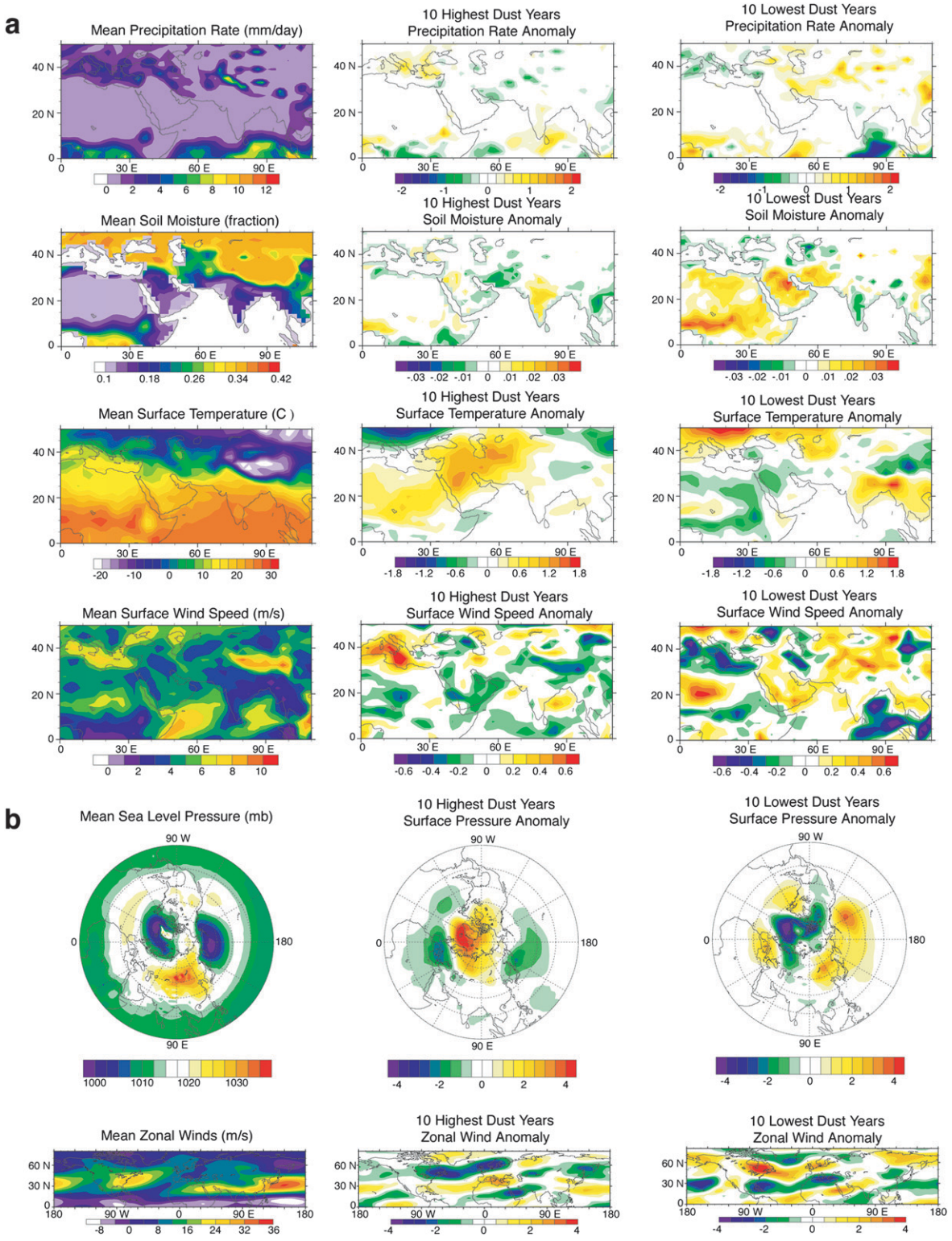

FIG. 8. (a) Mean winter (January–February) precipitation rate (mm day^{-1}), soil moisture (fraction), surface temperature (C°), and surface wind speed (m s^{-1}) from the NCEP reanalysis and their anomalies during the 10 highest and lowest dust years based on the mean annual Mount Everest Fe dust record from 1948 to 2001. (b) Mean winter (January–February) sea level pressure (mb) and 500-mb zonal winds (m s^{-1}) from the NCEP reanalysis and the surface pressure and 500-mb zonal wind anomalies during the 10 highest and lowest dust years based on the mean annual Mount Everest Fe dust record from 1948 to 2001.

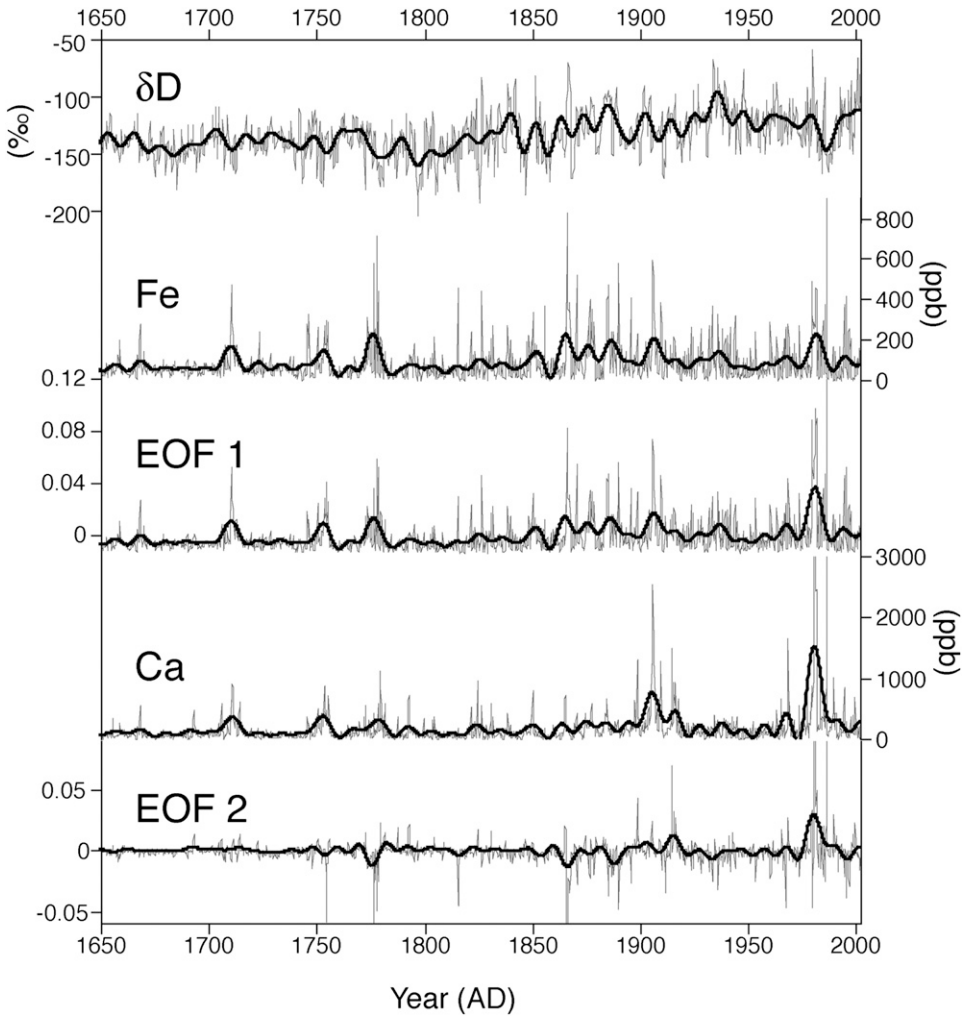

FIG. 9. Mount Everest δD, Fe, EOF1, Ca, and EOF2 data resampled to four samples per year (gray) with a 10-yr low-pass filter (black) from the period A.D. 1650–2000.

This change could be due to an increase in dust emissions in the source regions and/or enhanced transport of dust aerosols to the Himalayas. Dust particle concentrations (diameter >0.63 μm) in an ice core from the nearby Dasuopu glacier shows a similar increase since ca. A.D. 1860 (Thompson et al. 2000).

Synchronous with the dust increase is a shift to less negative δD and $\delta^{18}O$ in both the Everest and Dasuopu ice cores. Thompson et al. (2000) purport that $\delta^{18}O$ is a proxy for temperature in the Himalayas and that the increased dust levels and less negative $\delta^{18}O$ imply a link between warming and increased atmospheric dustiness due to decreased snow cover, increased aridity, and/or increased agricultural activities. This is consistent with our observation that temperatures in the dust source regions are higher during high dust years (Fig. 8). However, there are a number of factors in addition to temperature that can affect the stable isotopic composition of precipitation over the Himalayas, including relative humidity, condensation level, the amount effect, and moisture source regions (Tian et al. 2001). On seasonal time scales the isotopic composition of precipitation in the Himalayas is controlled by the amount effect (during which heavy isotopes are depleted relative to light isotopes during periods of high precipitation), not temperature, as δD is more negative during the summer monsoon season and less negative during the winter (Tian et al. 2003). There are multiple factors that may contribute to the synchronous relationship between dust concentrations and stable isotopes.

Variations in atmospheric circulation patterns, and hence moisture source regions, is one important factor that can affect the stable isotopic composition of

precipitation. Previous research on the major ion and δD records spanning the period A.D. 1000–2000 from the same Mount Everest ice core reported a shift to less negative δD at A.D. ~1400 (a period of time when temperatures were relatively cool) synchronous with an increase in continental (i.e., dust laden; Ca^{2+} used as a proxy for dust) air masses (Kaspari et al. 2007). Although the majority of precipitation is deposited at Mount Everest during the summer monsoon season, the synchronous timing of increased dust concentrations with less negative δD may be related to enhanced transport of continental air masses via the westerlies during the winter and a relative increase in winter contributions to the annual snow accumulation. If correct, this could indicate that the increase in dust concentrations since the 1800s is associated with a change in circulation resulting in enhanced dust transport. Other proxy records also suggest a shift in circulation at this time (Fisher et al. 2004; Mayewski et al. 2004).

The association of δD being less negative during periods of high dust concentrations is not consistent throughout the 350-yr record. For example, prior to 1800 there are three periods of high dust concentrations that do not coincide with less negative δD (Fig. 9). Periods of increased dust concentrations in the Himalayas are most likely the result of a combination of factors, including enhanced dust emissions in the dust source regions, changes in the atmospheric circulation patterns that result in more frequent transport of dust emissions to the Himalayan region, and episodic synoptic-scale events that can result in large dust storms. There is minimal information on past climate conditions in the dust source regions to determine if warmer temperatures or more arid conditions were an important factor in the increased dust emissions. Regardless of the cause, the knowledge of the timing and magnitude of these changes is valuable for future research investigating the impacts of dust on the climate system and biogeochemical and hydrological cycles.

g. *Potential impact of anthropogenic activities on atmospheric dust loading*

Anthropogenic activities including agriculture, overgrazing, deforestation, construction, and military activities in desert regions have the potential to increase dust emissions (Tegen et al. 2004; Mahowald et al. 2004). Results from previous attempts to estimate the global dust input from anthropogenically disturbed soils vary between studies suggesting minimal human impact on dust emissions (Prospero et al. 2002; Tegen et al. 2004) to studies reporting that anthropogenic dust sources could account for anywhere between 0% and 50% of dust emissions (Luo et al. 2003).

The Mount Everest ice core dust record was examined for evidence of increased dust emissions as a result of anthropogenic activities. The Everest Fe record indicates higher dust activity during the late 1970s–80s, but the increase is within the range of other periods of high dust activity during the 350-yr record (Fig. 9). However, it may be difficult to differentiate dust emissions from natural versus anthropogenic sources. For example, if dust inputs from anthropogenic sources occurred during a period of low dust inputs from natural sources, the atmospheric dust concentrations could still fall within the normal range. Nevertheless, there is not a detectable change in twentieth-century Fe concentrations that can be attributed uniquely to anthropogenic activities in the Everest record.

The highest Ca concentrations of the 350-yr record occur in the early 1900s and the late 1970s–80s, with two episodes of very large Ca inputs in 1980 and 1986 that are unprecedented in the 350-yr Everest Ca record (Fig. 9). Enrichment factor analysis on the same Everest ice core suggests that Ca is enriched relative to crustal elements in recent decades (Kaspari et al. 2009). As discussed earlier, Fe is a proxy for long-range dust sources, whereas Ca has significant long-range and local source inputs. That the Ca and EOF2 records show a late-twentieth-century increase, while the Fe record does not, suggests that any potential anthropogenic dust sources are from activities more proximal to Everest than the major dust sources.

The late-twentieth-century elevated Ca concentrations cannot be definitively attributed to anthropogenic dust emissions. Because the periods of high Ca concentrations are episodic, and concentrations during the 1990s are within the range of natural variability, the increase during the late 1970s–80s may be related to circulation changes or natural variations in dust emissions. However, the highest dust particle concentrations in the Dasuopu ice core record occur since the ~1950s, and anthropogenic activities may be the cause of this increase (Thompson et al. 2000). Further research is needed to understand how the trace element chemistry varies with dust particle concentrations. However, as stated previously, if the source of the increased dust concentrations is anthropogenic, the Everest Ca data suggests that the geographic source of the dust would be from regions more proximal to Everest (as opposed to the major dust source regions, such as the Arabian Peninsula, North Africa, and/or the Thar Desert). Detectable anthropogenic inputs of dust emissions are more likely to originate from nondesert regions that are vulnerable to desertification, such as the margins of the Thar Desert, or regions of southern

Nepal and northern India (Tewari and Arya 2005) (e.g., http://soils.usda.gov/use/worldsoils/mapindex/desert.html; U.S. Department of Agriculture, Natural Resources Conservation Service, Soil Survey Division, World Soil Resources). The Mount Everest and Dasuopu ice core records provide a basis for understanding atmospheric dust concentrations. By continuing to monitor atmospheric dust concentrations and collecting more Asian ice core dust records, the anthropogenic contribution to atmospheric dust emissions can be more clearly assessed.

4. Summary and conclusions

The Mount Everest ice core record provides the first high-resolution, continuous record of trace element concentrations from an Asian ice core spanning the preindustrial to modern time period. This record was used to investigate variations in the chemical composition of dust and atmospheric dust concentrations from the period A.D. 1650–2000. There are large seasonal variations in the dust loading of the atmosphere over this region with peak dust concentrations occurring during the winter months. The chemical composition of dust differs between low and high dust periods, indicating seasonal differences in the dominant source of dust.

Our results suggest that the Arabian Peninsula, Thar Desert, and northern Sahara are the dominant sources of dust deposited during the winter months at Everest. Back-trajectory analysis verifies the atmospheric transport pathways by which dust aerosols can be transported from these dust source areas to the Everest region.

Numerous factors control atmospheric dust concentrations, including dust generation at the surface and the strength and pathways of winds that transport dust aerosols. A comparison of the Everest dust records with the NCEP reanalysis suggests that increased soil moisture decreases dust emissions, while warmer temperatures cause an increase in dust emissions. Mean surface wind speeds in the dust source regions do not appear to be associated with dust emissions. The reason for this may be that strong wind conditions at the surface only need to occur episodically to entrain dust aerosols into the atmosphere, and the NCEP data considered represent mean seasonal conditions. Additionally, sustained dry or warm periods could be more important than wind speed in creating conditions favorable for increased dust emissions. However, because of limitations in the reanalysis data, these findings are not definitive.

There are periods of high dust concentrations throughout the 350-yr Mount Everest dust record; however, there are more frequent periods of high dust concentrations since the early 1800s. This increase is likely a consequence of both increased dust emissions in the source regions and more effective transport of the dust aerosols to the Everest region. Knowledge of the timing and magnitude of these dust increases may be useful in future research investigating the impacts of dust on the climate system and biogeochemical and hydrological cycles.

Anthropogenic activities may result in increased dust emissions (Tegen et al. 2004). An examination of the Everest record for evidence of increased dust emissions related to anthropogenic activities indicates no apparent change in twentieth-century concentrations of Fe, representative of dust from the dominant dust source regions (Arabian Peninsula, Thar Desert, and northern Sahara). Periods of increased Ca concentrations during the twentieth century could be due to dust emissions from anthropogenic activities in regions vulnerable to desertification, but our results are inconclusive. Because of the high elevation of the Everest drill site and its location downwind of major dust sources, the Everest drill site may not be the best location to assess anthropogenic contributions to atmospheric dust concentrations. Further studies and monitoring of dust concentrations are necessary to assess the impact of anthropogenic activities on atmospheric dust concentrations. Particular attention should be paid to changes in dust emissions in a warming climate; our results suggest a strong association between higher temperatures and dust emissions (Fig. 8a). However, some model simulations predict that future (A.D. 2090) dust emissions may be lower than current levels under future climate conditions (Mahowald and Luo 2003). The Mount Everest ice core record provides a valuable baseline record with which to compare future dust emissions.

The Mount Everest ice core record is the most detailed Asian dust record of its kind. Analysis of the record has improved our understanding of variations in the composition and concentrations of atmospheric dust through time, the dominant dust sources and transport pathways, and the dominant controls on dust generation. However, additional dust records similar to the Mount Everest record are needed from spatially distributed sites to gain a more comprehensive understanding of spatial and temporal dust variability and its associated impacts.

Acknowledgments. This research was funded by NSF ATM 0139491, NOAA NA05OAR4311109, the Natural Science Foundation of China (90411003, 40401054), and the Chinese Academy of Sciences (''Talents Project'' and the Innovation Programs: KZCX3-SW-339/344).

REFERENCES

Duce, R. A., 1995: Sources, distribution and fluxes of mineral aerosols and their relationship to climate. *Aerosol Forcing on Climate,* R. J. Carlson and J. Heintzenberg, Eds., J. Wiley, 43–72.

Engelstaedter, S., K. E. Kohfeld, I. Tegen, and S. P. Harrison, 2003: Controls of dust emissions by vegetation and topographic depressions: An evaluation using dust storm frequency data. *Geophys. Res. Lett.,* **30,** 1294, doi:10.1029/2002GL016471.

Fisher, D. A., and Coauthors, 2004: Stable isotope records from Mount Logan, eclipse ice cores, and nearby Jellybean Lake. Water cycle of the North Pacific over 2000 years and over five vertical kilometers: Sudden shifts and tropical connections. *Geogr. Phys. Quat.,* **58,** 337–352.

Giaveri, G., and Coauthors, 2005: INAA at the top of the world: Elemental characterization and analysis of airborne particulate matter collected in the Himalayas at 5,100 m high. *J. Radioanal. Nucl. Chem.,* **263,** 725–732.

Goudie, A. S., and N. J. Middleton, 1992: The changing frequency of dust storms through time. *Climatic Change,* **20,** 197–225.

Griffin, D. W., and C. A. Kellogg, 2004: Dust storms and their impact on ocean and human health: Dust in Earth's atmosphere. *EcoHealth,* **1,** 284–295.

Hurrel, J. W., Y. Kushhir, M. Visbeck, and G. Ottersen, 2003: An overview of the North Atlantic Oscillation. *The North Atlantic Oscillation: Climate Significance and Environmental Impact, Geophys. Monogr.,* Vol. 134, Amer. Geophys. Union, 1–35.

Jickells, T. D., and Coauthors, 2005: Global iron connections between desert dust, ocean biogeochemistry, and climate. *Science,* **308,** 67–71.

Kalnay, E., and Coauthors, 1996: The NCEP/NCAR 40-Year Reanalysis Project. *Bull. Amer. Meteor. Soc.,* **77,** 437–471.

Kang, S., P. A. Mayewski, D. Qin, Y. Yan, S. Hou, D. Zhang, and K. J. Kreutz, 2002: Glaciochemical records from a Mt. Everest ice core: Relationship to atmospheric circulation over Asia. *Atmos. Environ.,* **36,** 3351–3361.

——, ——, ——, S. Sneed, J. Ren, and D. Zhang, 2004: Seasonal differences in snow chemistry from the vicinity of Mt. Everest, central Himalayas. *Atmos. Environ.,* **38,** 2819–2829.

Kaspari, S., and Coauthors, 2007: Reduction in northward incursions of the South Asian Monsoon since ~1400 AD inferred from a Mt. Everest ice core. *Geophys. Res. Lett.,* **34,** L16701, doi:10.1029/2007GL030440.

——, R. Hooke, P. A. Mayewski, S. Kang, S. Hou, and D. Qin, 2008: Snow accumulation rate on Qomolangma (Mount Everest), Himalaya: Synchroneity with sites across the Tibetan Plateau on 50-100 year timescales. *J. Glaciol.,* **54,** 343–352.

——, P. A. Mayewski, M. Handley, E. Osterberg, S. Kang, S. Sneed, S. Hou, and D. Qin, 2009: Recent Increases in atmospheric concentrations of Bi, U, Cs, S and Ca from a 350-year Mt. Everest ice core record. *J. Geophys. Res.,* **114,** D04302, doi:10.1029/2008JD011088.

Kreutz, K. J., and E. R. Sholkovitz, 2000: Major element, rare earth element, and sulfur isotopic composition of a high-elevation firn core: Sources and transport of mineral dust in Central Asia. *Geochem. Geophys. Geosyst.,* **1,** 1048, doi:10.1029/2000GC000082.

Li, Y., T. Yao, N. Wang, Z. Li, L. Tian, B. Xu, and G. Wu, 2006: Recent changes of atmospheric heavy metals in a high elevation ice core from Muztagh Ata in East Pamirs: Initial results. *Ann. Glaciol.,* **43,** 154–159.

Luo, C., N. M. Mahowald, and J. del Corral, 2003: Sensitivity study of meteorological parameters on mineral aerosol mobilization, transport, and distribution. *J. Geophys. Res.,* **108,** 4447, doi:10.1029/2003JD003483.

Mahowald, N. M., and C. Luo, 2003: A less dusty future? *Geophys. Res. Lett.,* **30,** 1903, doi:10.1029/2003GL017880.

——, and J.-L. Dufresne, 2004: Sensitivity of TOMS aerosol index to boundary layer height: Implications for detection of mineral aerosol sources. *Geophys. Res. Lett.,* **31,** L03103, doi:10.1029/2003GL018865.

——, G. D. Rivera Rivera, and C. Luo, 2004: Comment on ''Relative importance of climate and land use in determining present and future global soil dust emission'' by I. Tegen et al. *Geophys. Res. Lett.,* **31,** L24105, doi:10.1029/2004GL021272.

Mayewski, P. A., and Coauthors, 2004: A 700 year record of Southern Hemisphere extratropical climate variability. *Ann. Glaciol.,* **39,** 127–132.

Middleton, N. J., 1986: A geography of dust storms in south-west Asia. *Int. J. Climatol.,* **6,** 183–196.

Miller, R. L., and I. Tegen, 1998: Climate response to soil dust aerosols. *J. Climate,* **11,** 3247–3267.

Osterberg, E. C., M. J. Handley, S. Sneed, P. A. Mayewski, and K. J. Kreutz, 2006: Continuous ice core melter system with discrete sampling for major ion, trace element, and stable isotope analyses. *Environ. Sci. Technol.,* **40,** 3355–3361.

Prospero, J. M., M. Uematsu, and D. L. Savoie, 1989: Mineral aerosol transport to the Pacific Ocean. *Chemical Oceanography,* J. P. Riley, R. Chester, and R. A. Duce, Eds., Academic, 188–218.

——, P. Ginoux, O. Torres, S. E. Nicholson, and T. E. Gill, 2002: Environmental characterization of global sources of atmospheric soil dust identified with the Nimbus 7 Total Ozone Mapping Spectrometer (TOMS) absorbing aerosol product. *Rev. Geophys.,* **40,** 1002, doi:10.1029/2000RG000095.

Rosenfeld, D., Y. Rudich, and R. Lahav, 2001: Desert dust suppressing precipitation: A possible desertification feedback loop. *Proc. Natl. Acad. Sci. USA,* **98,** 5975–5980.

Solomon, S., D. Qin, M. Manning, Z. Chen, M. Marquis, K. B. Averyt, M. Tignor, and H. L. Miller, 2007: *Climate Change 2007: The Physical Science Basis*. Cambridge University Press, 996 pp.

Song, Y., T. Zhu, X. Cai, W. Lin, and L. Kang, 2007: Glacier winds in the Rongbuk Valley, north of Mount Everest: 1. Meteorological modeling with remote sensing data. *J. Geophys. Res.,* **112,** D11101, doi:10.1029/2006JD007867.

Tegen, I., M. Werner, S. P. Harrison, and K. E. Kohfeld, 2004: Relative importance of climate and land use in determining present and future global soil dust emission. *Geophys. Res. Lett.,* **31,** L05105, doi:10.1029/2003GL019216.

Tewari, V. P., and R. Arya, 2005: Degradation of arid rangelands in Thar Desert, India: A review. *Arid Land Res. Manage.,* **19,** 1–12.

Thompson, L. G., T. Yao, E. Mosley-Thompson, M. Davis, B. Henderson, and P. N. Lin, 2000: A high-resolution millennial record of the South Asian Monsoon from Himalayan ice cores. *Science,* **289,** 1916–1919.

Tian, L., V. Masson-Delmotte, M. Stievenard, T. Yao, and J. Jouzel, 2001: Tibetan Plateau summer monsoon northward extent revealed by measurements of water stable isotopes. *J. Geophys. Res.,* **106,** 28 081–28 088.

——, T. Yao, P. F. Schuster, J. W. C. White, K. Ichiyanagi, E. Pendall, J. Pu, and W. Yu, 2003: Oxygen-18 concentrations in recent precipitation and ice cores on the Tibetan Plateau. *J. Geophys. Res.,* **108,** 4293, doi:10.1029/2002JD002173.

Torres, O., P. K. Bhartia, J. R. Herman, and Z. Ahmad, 1998: Derivation of aerosol properties from satellite measurements of backscattered ultraviolet radiation. *J. Geophys. Res.,* **103,** 17 099–17 110.

——, ——, ——, A. Sinyuk, P. Ginoux, and B. Holben, 2002: A long-term record of aerosol optical depth from TOMS observations and comparison to AERONET measurements. *J. Atmos. Sci.,* **59,** 398–413.

Wake, C. P., P. A. Mayewski, X. Zichu, W. Ping, and L. Zhongqin, 1993: Regional distribution of monsoon and dust signals in Asian glaciers. *Geophys. Res. Lett.,* **20,** 1411–1414.

——, J. Dibb, P. A. Mayewski, P. A. Xie, and Z. Li, 1994: The chemical composition of aerosols over the eastern Himalaya and Tibetan Plateau during low dust period. *Atmos. Environ.,* **28,** 695–704.

Washington, R., M. Todd, N. J. Middleton, and A. S. Goudie, 2003: Dust-storm source areas determined by the Total Ozone Monitoring Spectrometer and surface observations. *Ann. Assoc. Amer. Geogr.,* **93,** 297–313.

Zender, C. S., and E. U. Kwon, 2005: Regional contrasts in dust emission responses to climate. *J. Geophys. Res.,* **110,** D13201, doi:10.1029/2004JD005501.

Zhang, D., 1985: Meteorological characteristics of dust fall in China since the historic times. *Quaternary Geology and Environment of China,* T. S. Liu, Ed., China Ocean Press, 101–106.

Zhang, X., R. Arimoto, J. Cao, Z. An, and D. Wang, 2001: Atmospheric dust aerosol over the Tibetan Plateau. *J. Geophys. Res.,* **106,** 18 417–18 476.